Short Papers

A Simplified Field Analysis of a Distributed IMPATT Diode Using Multiple Uniform Layer Approximation

MASAYUKI MATSUMOTO, MEMBER, IEEE, MAKOTO TSUTSUMI, MEMBER, IEEE, AND NOBUAKI KUMAGAI, FELLOW, IEEE

Abstract — **A small-signal field analysis of a distributed IMPATT diode is presented. The active region of the diode is assumed to consist of a uniform avalanche layer and avalanche-free drift layers. The propagation constant and field distributions are obtained without numerical solution of differential equations, which is necessary in the analysis described in [9]. Some numerical results are given which show the dependence of the amplification characteristics on the thickness of the avalanche and drift layers.**

I. Introduction

Amplification characteristics of traveling-wave modes in slab-like distributed IMPATT diodes have recently been studied both theoretically and experimentally with the intent of realizing IMPATT oscillators having large device area or two-port IMPATT amplifiers [1]–[10].

In the previous field analysis presented by Fukuoka and Itoh [9], a set of differential equations must be solved numerically to obtain the propagation constant and field distributions. In this paper, we present a simplified small-signal field analysis of distributed IMPATT diodes using the multiple uniform layer approximation [11], where the active region of the diode is assumed to consist of a uniform avalanche layer and avalanche-free drift layers. The effects of losses caused by the presence of inactive layers are included in the analysis. Some numerical examples of GaAs double-Read distributed IMPATT diodes are given which show the dependence of the amplification characteristics on the thicknesses of the constituent layers.

II. Formulation of the Problem

Fig. 1 shows the side view of a two-dimensional ($\partial/\partial y = 0$) distributed IMPATT diode analyzed in this paper. The active region ($0 < x < d_1 + w + d_2$) is assumed to consist of two avalanche-free drift layers and, between them, an avalanche layer having a constant ionization rate. The assumption of constant avalanche is equivalent to assuming that the dc electric field is distributed uniformly across the avalanche layer, which can be approximately realized in double-Read IMPATT structures [10] having doping spikes at the boundaries between the drift and avalanche layers. The active region is covered by heavily doped p^+, n^+ layers and metal layers. These inactive layers are treated as lossy dielectric layers having finite conductivities.

With the small-signal assumptions, we can obtain a set of differential equations governing the ac components of the electric field and the electron and hole current densities in the x-direction

Manuscript received January 14, 1988; revised March 14, 1988

M Matsumoto and M Tsutsumi are with the Department of Communication Engineering, Faculty of Engineering, Osaka University, Suita, Osaka 565, Japan

N Kumagai was with the Department of Communication Engineering, Osaka University. He is now President of Osaka University.

IEEE Log Number 8821763.

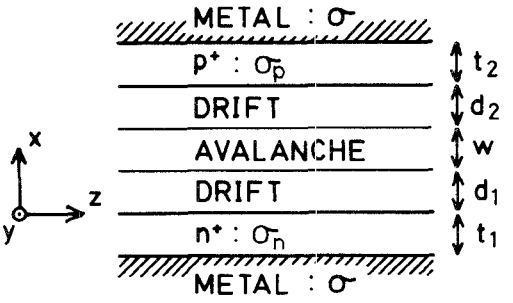

Fig. 1 Side view of the distributed IMPATT diode analyzed in this paper

in the avalanche layer ($d_1 < x < d_1 + w$) as follows:

$$\frac{\partial^2 E_x}{\partial x^2} + \left(\omega^2\epsilon_0\mu_0\epsilon_r + \gamma^2\right)E_x + \frac{1}{\epsilon_0\epsilon_r v_s}\left(\frac{\partial J_{nx}}{\partial x} - \frac{\partial J_{px}}{\partial x}\right) - j\omega\mu_0\left(J_{nx} + J_{px}\right) = 0 \quad (1a)$$

$$\frac{\partial J_{nx}}{\partial x} = \left(\frac{j\omega}{v_s} - \alpha_{dc}\right)J_{nx} - \alpha_{dc}J_{px} - \alpha' J_{dc}E_x \quad (1b)$$

$$\frac{\partial J_{px}}{\partial x} = \alpha_{dc}J_{nx} - \left(\frac{j\omega}{v_s} - \alpha_{dc}\right)J_{px} + \alpha' J_{dc}E_x \quad (1c)$$

where

- ϵ_0 free-space permittivity,
- μ_0 free-space permeability,
- ϵ_r relative permittivity of the semiconductor,
- ω angular frequency,
- γ propagation constant in the z direction (ac components of the fields have a factor of $\exp[j\omega t - \gamma z]$),
- v_s saturation velocity of carriers
- $\alpha(E)$ ionization rate ($\alpha_{dc} = \alpha(E_{dc}) = 1/w$, $\alpha' = \left.\frac{d\alpha}{dE}\right|_{E=E_{dc}}$),
- J_{dc} dc bias current density.

In deriving (1), we have made use of the following simplifying assumptions: 1) ionization rates for electrons and holes are equal, 2) saturation velocities of electrons and holes are equal, 3) diffusion currents are neglected, and 4) conductivity in the z direction is zero ($J_{nz} = J_{pz} = 0$ while E_z is present). In drift layers, the same equation as (1) but with $\alpha_{dc} = \alpha' = 0$ holds.

Since (1) comprises a set of linear differential equations having constant coefficients, it can be solved analytically, resulting in the form

$$E_x = \sum_{i=1}^{4} A_i \exp(k_i x) \quad (2a)$$

$$J_{nx} = \sum_{i=1}^{4} A_i B_i \exp(k_i x) \quad (2b)$$

$$J_{px} = \sum_{i=1}^{4} A_i C_i \exp(k_i x) \quad (2c)$$

where the A_i's are unknown constants and the k_i's are the

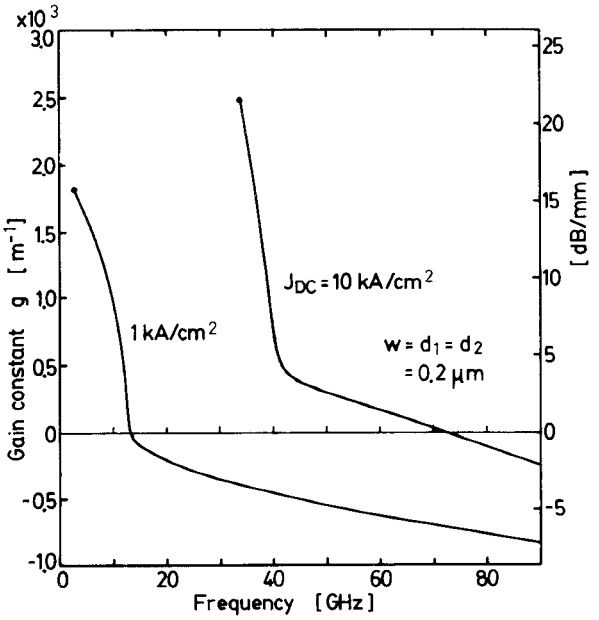

Fig. 2. Frequency characteristics of the gain constant

solutions of the biquadratic equation

$$k^4+\left(\gamma^2+\omega^2\epsilon_0\mu_0\epsilon_r+\frac{2j\omega\alpha_{dc}}{v_s}+\frac{\omega^2}{v_s^2}-\frac{2\alpha' J_{dc}}{\epsilon_0\epsilon_r v_s}\right)k^2$$
$$+\left(\gamma^2+\omega^2\epsilon_0\mu_0\epsilon_r\right)\left(\frac{2j\omega\alpha_{dc}}{v_s}+\frac{\omega^2}{v_s^2}\right)-\frac{2\omega^2\mu_0\alpha' J_{dc}}{v_s}=0$$

and

$$B_t=-\alpha' J_{dc}\left(k_t+\frac{j\omega}{v_s}\right)\Bigg/\left(k_t^2+\frac{2j\omega\alpha_{dc}}{v_s}+\frac{\omega^2}{v_s^2}\right)$$

$$C_t=\alpha' J_{dc}\left(k_t-\frac{j\omega}{v_s}\right)\Bigg/\left(k_t^2+\frac{2j\omega\alpha_{dc}}{v_s}+\frac{\omega^2}{v_s^2}\right).$$

Other field components in the active layers are expressed in terms of E_x, J_{nx}, and J_{px} by

$$E_z=\frac{1}{\gamma}\left\{\frac{\partial E_x}{\partial x}+\frac{1}{\epsilon_0\epsilon_r v_s}\left(J_{nx}-J_{px}\right)\right\} \tag{3a}$$

$$H_y=\frac{1}{\gamma}\left(J_{nx}+J_{px}+j\omega\epsilon_0\epsilon_r E_x\right) \tag{3b}$$

which are derived from Maxwell's equations.

The electromagnetic field expressions in inactive layers ($x<0$, $d_1+w+d_2<x$) can be obtained by solving source-free Maxwell's equations with complex relative permittivity $\epsilon_t=\epsilon_r-j\sigma_t/(\omega\epsilon_0)$ as has been done in [9].

Applying the boundary conditions

1) E_z and H_y are continuous throughout the structure,
2) J_{nx} and J_{px} are continuous at $x=d_1$ and $x=d_1+w$,
3) $J_{px}=0$ at $x=0$,
4) $J_{nx}=0$ at $x=d_1+w+d_2$,

to the general solutions of the constituent layers yields a set of homogeneous linear equations which can be written in a matrix form as $\mathbb{A}x=\mathbb{0}$, where $\mathbb{A}$ is a coefficient square matrix and x is a vector composed of unknown constants such as the A_t's given in (2). By solving the characteristic equation $\det[\mathbb{A}(\gamma)]=0$, we can obtain the propagation constant, and from the solution for the vector x we can calculate field distributions using (2) and (3).

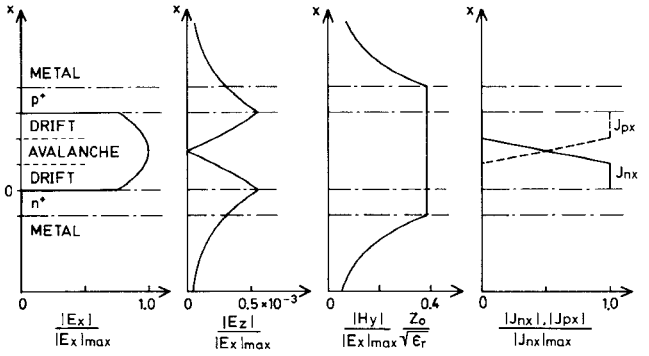

Fig 3 Field and current distributions ($w=d_1=d_2=0.2$ μm, $J_{dc}=10$ kA/cm², $f=50$ GHz).

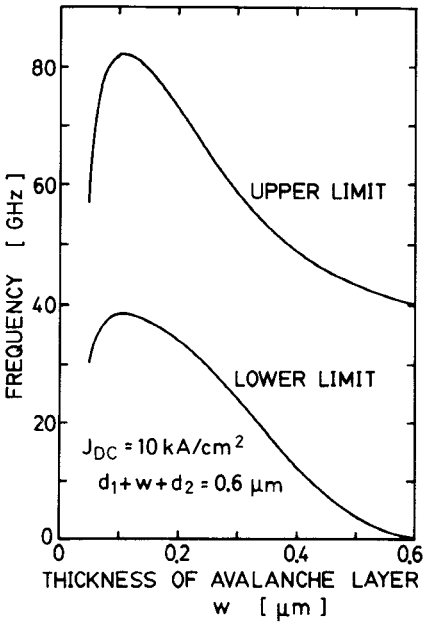

Fig 4 Frequency range of amplification versus the avalanche-layer thickness

III. Numerical Examples

We have made numerical calculations assuming GaAs with $\epsilon_r=12.9$, $v_s=6\times10^4$ m/s, and $\alpha(E)=3.5\times10^7\exp\{-(6.85\times10^7/E)^2\}$ m^{-1} (E in V/m) as the semiconductor material. Thicknesses and conductivities of p^+ and n^+ layers are $t_1=t_2=0.2$ μm, $\sigma_p=2.03\times10^4$ S/m, and $\sigma_n=4.31\times10^5$ S/m. These conductivities correspond to impurity concentrations $N_A=N_D=3.16\times10^{18}$ cm^{-3} when mobilities $\mu_e=8500$ cm²/Vs and $\mu_h=400$ cm²/Vs are assumed. Metal layers outside the semiconductor layers are assumed to be copper, with $\sigma=5.8\times10^7$ S/m.

Fig. 2 shows a typical example of the frequency characteristics of the gain constant $g=-\mathrm{Re}[\gamma]$. In this figure, the phase constant $\beta=\mathrm{Im}[\gamma]$ becomes zero at $f=3$ GHz and 34 GHz for $J_{dc}=1$ kA/cm² and 10 kA/cm², respectively, and below these frequencies no amplification is obtained. Fig. 3 shows field and current distributions at $f=50$ GHz ($J_{dc}=10$ kA/cm²) where the gain constant is 2.61 dB/mm.

In fig. 4 we show a plot of the frequency range where the gain constant is positive as a function of the avalanche-layer thickness with the whole active-layer thickness kept constant. The upper and lower frequency limits of the range have peaks at $w=0.11$

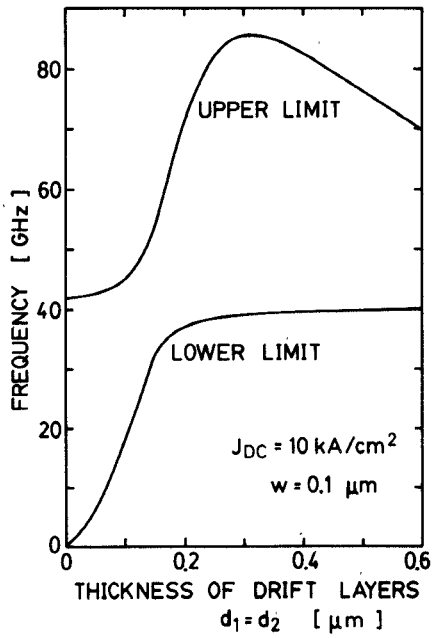

Fig. 5. Frequency range of amplification versus the drift-layer thickness.

μm, near the point where the avalanche resonance frequency of the avalanche layer [11] takes the highest value. Fig. 5 shows the frequency range of amplification against the drift-layer thickness with the avalanche-layer thickness kept constant. For the thicknesses below $d_1 = d_2 = 0.3$ μm, the upper frequency limit decreases with decreasing $d_1 = d_2$. This is because the relative amount of power dissipated in the inactive layers is larger for smaller active-layer thickness.

IV. Conclusions

We have presented a simplified field analysis of a distributed IMPATT diode in the traveling-wave mode using a multiple uniform layer approximation.

In order to understand thoroughly the operation of distributed IMPATT oscillators and amplifiers and to solve the problem of coupling these devices with other circuit components, the behavior of electromagnetic fields at the diode facets must be known. The IMPATT diode model presented in this paper will be useful for the analysis of these discontinuity problems.

Acknowledgment

The authors wish to thank Y. Yamaguchi for his assistance in this work.

References

[1] T. A. Midford and H. C. Bowers, "A two-port IMPATT diode traveling wave amplifier," *Proc. IEEE*, vol. 56, pp. 1724–1725, Oct. 1968.

[2] N. S. Davydova, Yu. Z. Danyushevskiy, and L. I. Telyatnikov, "Linear theory of an IMPATT diode distributed microwave amplifier," *Telecommun. Radio Eng.*, pt. 2, vol. 27, pp. 112–115, Aug 1972.

[3] K. G. Hambleton and P. N. Robson, "Design considerations for resonant traveling wave IMPATT oscillators," *Int. J. Electron.*, vol. 35, pp. 225–244, Aug. 1973.

[4] M. Franz and J. B. Beyer, "The traveling-wave IMPATT mode," *IEEE Trans. Microwave Theory Tech.*, vol. MTT-26, pp 861–865, Nov. 1978

[5] M. Franz and J. B. Beyer, "The traveling wave IMPATT mode: Part II—The effective wave impedance and equivalent transmission line," *IEEE Trans. Microwave Theory Tech.*, vol. MTT-28, pp. 215–218, Mar. 1980.

[6] J. Soohoo, "Gain characteristics of a distributed IMPATT device," *IEEE Trans. Electron Devices*, vol. ED-30, pp. 1405–1406, Oct. 1983.

[7] B. Bayraktaroglu and H. D. Shih, "Millimeter-wave GaAs distributed IMPATT diodes," *IEEE Electron Device Lett.*, vol. EDL-4, pp. 393–395, Nov. 1983.

[8] B Bayraktaroglu and H. D. Shih, "A GaAs distributed IMPATT diode amplifier," *IEEE Electron Device Lett.*, vol. EDL-5, pp 466–467, Nov 1984.

[9] Y. Fukuoka and T. Itoh, "Field analysis of a millimeter-wave GaAs double-drift IMPATT diode in the traveling-wave mode," *IEEE Trans Microwave Theory Tech.*, vol. MTT-33, pp. 216–222, Mar. 1985.

[10] R. K. Mains and G. I. Haddad, "Traveling-wave IMPATT amplifiers and oscillators," *IEEE Trans. Microwave Theory Tech*, vol MTT-34, pp. 965–971, Sept. 1986.

[11] T. Misawa, "Multiple uniform layer approximation in analysis of negative resistance in p-n junction in breakdown," *IEEE Trans. Electron Devices*, vol. ED-14, pp. 795-808, Dec. 1967.

The Effects of a Dielectric Capacitor Layer and Metallization on the Propagation Parameters of Coplanar Waveguide for MMIC

R. DELRUE, C. SEGUINOT, P. PRIBETICH, AND P. KENNIS

***Abstract*—The study of coupling phenomena between lines laid on semiconductor substrates in MMIC technologies and the determination of propagation effects on power FET require the characterization lines with micron transversal widths. For such lines, the influence of metallization thickness and dielectric cap layer on propagation properties can no longer be neglected. The purpose of this paper is to characterize these effects for the case of coplanar lines laid on semiconductor substrates.**

I. Introduction

In the past, numerous lines laid on dielectric substrate have been studied, leading to the determination of the basic parameters (the attenuation and the phase constant) by means of various analytical and numerical techniques such as conformal mapping, finite element, finite difference, mode matching, and the spectral-domain approach. More recently, planar metal insulator semiconductor (MIS) or Schottky contact structures have been investigated by several authors [1]–[5] using the different kinds of numerical techniques.

In this paper we study the combined influence of thickness metallization and dielectric capacitor layer on the propagation parameters of coplanar lines on various semi-insulating or semiconductor substrates. The mathematical development used and the results which can be obtained by this numerical technique are presented.

II. Method

In order to take into account the most physical parameters and effects, we have studied the structures shown in Fig. 1(a) and (b) (a conductor-backed coplanar waveguide [1]) using the mode matching technique as in [3]. We consider the relative complex permittivity for each layer of the structure and the hybrid nature of the mode.

In this paper we focus our attention on the even dominant mode, so a magnetic wall is placed at $X = 0$, the symmetry axis of the structure.

The method used requires the division of the cross-sectional structure into subdomains in which the fields are expanded in a set of eigenfunctions relative to each subdomain (Fig. 1(c)). In

Manuscript received October 9, 1987; revised March 1, 1988.

The authors are with the Centre Hyperfrequences et Semiconducteurs U.A. CNRS No. 287, Universite des Sciences et Techniques de Lille, Flandres, Artois, 59655 Villeneuve d'Ascq, France.

IEEE Log Number 8821762.